Jiin-Jyh Shyu* and Pei-Chun Tsai

Preparation and characterization of stannous phosphate glass – polytetrafluoroethylene composites

https://doi.org/10.1515/ijmr-2023-0237 Received August 3, 2023; accepted January 4, 2024; published online April 26, 2024

Abstract: A low- $T_{\rm g}$ SnO-MgO-P₂O₅ (SMP) glass was mixed with polytetrafluoroethylene (PTFE) to form composites by a sintering route. Effects of SMP:PTFE ratio and sintering temperature (350 °C-430 °C) on the microstructure and the bonding ability to a low thermal-expansion glass substrate were investigated. The onset softening temperatures of SMP and PTFE are close (328 °C and 313 °C), which are much lower than the onset temperature of weight loss of PTFE (381 °C). This is important for the sintering of SMP-PTFE composites. After sintering, pure SMP glass was not able to bond to the low thermal-expansion 1737® glass substrates. However, SMP-PTFE composites were able to bond to 1737® after sintering at appropriate temperatures. A possible mechanism for the enhancement of bonding by adding PTFE is discussed.

Keywords: $SnO-P_2O_5$ glass; Polytetrafluoroethylene; Sintering

1 Introduction

Glass systems based on PbO–ZnO–B₂O₃,^{1,2} SnO–P₂O₅,^{3,4} Bi₂O₃–ZnO–B₂O₃,⁵ and V₂O₅–TeO₂–P₂O₅,⁶ etc., exhibit low glass transition temperatures (T_g) and acceptable chemical durability. Therefore, these low- T_g glasses can be used as sealing materials for joining different parts that can not be processed at high temperatures, e.g., electronic devices. The typical joining/sealing temperatures can be lower than, e.g., 450 °C.

One of the disadvantages of low- $T_{\rm g}$ sealing glasses is that their coefficients of thermal expansion (*CTE*), e.g.,

 $100-120 \times 10^{-7}~K^{-1}$ for SnO–ZnO– P_2O_5 glasses,³ are much higher than several important low-*CTE* materials such as silicon ($CTE=37\times 10^{-7}~K^{-1}$). The high discrepancy in *CTE* would result in remarkable thermal stresses during cooling after the sintering process. One method to reduce the *CTE* of sealing glass is to incorporate low-*CTE* filler phases, e.g., high-quartz solid solutions, β -eucryptite, β -spodumene, cordierite, silica glass.⁴ However, addition of these refractory filler addition of these refractory filler reduces the sinterability of the glass powder.

Similar to the above-mentioned low- T_g sealing glasses, thermoplastic polymers can also be softened at low temperatures. Compared to sealing glasses, polymers offer several advantages, including high flexibility, easy processing, and low cost, etc. Therefore, it would be of great interest to explore the formation and characteristics of such a composite material by incorporating a polymer with a softening temperature similar to that of the low- T_g glass. Nevertheless, polymers generally have lower service temperatures compared to glasses. Polytetrafluoroethylene (PTFE composites) is a thermoplastic polymer with high crystallinity, high chemical resistance, high melting point (327 °C^{7,8}), and high decomposition temperature.9-11 It also exhibits good flexibility,12 low dielectric permittivity, low loss tangent, and high strength of dielectric breakdown. 13,14 Based on its excellent properties, PTFE and PTFE-based composites have been used for various applications, e.g., insulation, capacitors, 15 and substrate materials for communication technology. 16-25 Several refractory materials, including crystalline ceramics^{18-21,23-25} and glasses,^{17,22,26} have been distributed over PTFE matrix to modify the thermal, chemical, and dielectric properties of the composites. Ceramic-PTFE composites with high ceramic contents have also been studied.²⁶ However, few studies have been made to prepare and characterize composites containing low- $T_{
m g}$ glasses and PTFE. The low sintering-temperature of the low- T_g glass is helpful to avoid thermal decomposition or degradation of PTFE during sintering.

Glasses in the SnO–MgO– P_2O_5 system exhibit low T_g , high CTE, and good chemical durability.^{27–29} In the present paper, PTFE was distributed over the low- T_g 60SnO-10MgO-30 P_2O_5 (mol.% SMP) glass to form glass-based composites by

^{*}Corresponding author: Jiin-Jyh Shyu, Department of Mechanical and Materials Engineering, Tatung University, Taipei 104, Taiwan, E-mail: jjshyu@gm.ttu.edu.tw. https://orcid.org/0000-0002-6125-8377

Pei-Chun Tsai, Department of Mechanical and Materials Engineering, Tatung University, Taipei, Taiwan

a sintering route. It is interesting to see whether such sealing materials are able to bond to a low thermal-expansion material or not. It is expected that the thermal stresses developed by the CTE mismatch between SMP glass and low thermal-expansion materials can be relaxed with the aid of the flexibility of the PTFE phase.

2 Experimental procedures

2.1 Preparation of glass powder

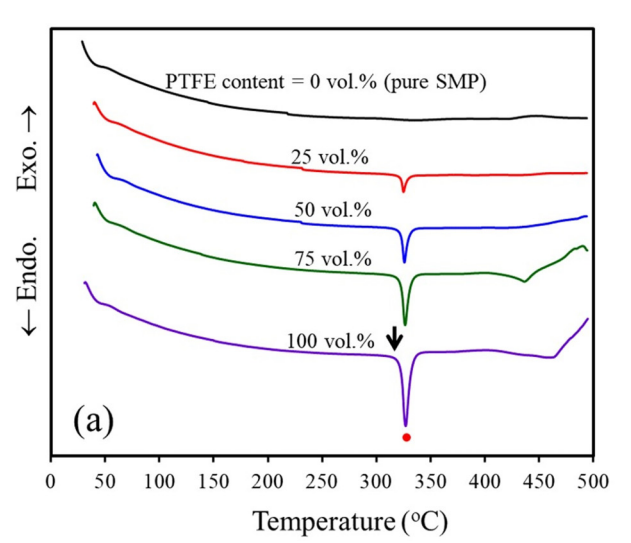
Glass powder of composition 60SnO-10MgO-30P₂O₅ (mol.%) was prepared. Reagent-grade raw materials Sn₂P₂O₇ and MgO were mixed, followed by being melted in an alumina crucible at 975 °C for 20 min. Glass frits were obtained by quenching the liquid into deionized water. A mix-mill machine (model MM2000, Retsch GmbH, Haan, Germany) was used to reduce the particle size of the glass powder. The resulting particle size of 37-44 µm was obtained by sieving, denoted as SMP.

2.2 Preparation of glass-PTFE composites

The SMP powder was mixed with various amounts of PTFE powder in a mix-mill machine. The mixed powders were pressed into disc-shaped green compacts (diameter 5 mm). The powder compact was placed between an upper and a bottom Corning 1737® glass substrate, then was sintered for 10 min at 350 °C-430 °C in air. The heating rate was 10 K min⁻¹.

2.3 Characterization

Phase-transition temperatures of the SMP-PTFE powder mixtures were examined by thermogravimetric analysis and differential thermal



analysis (TGA-DTA, model SDT2960, TA Instruments, New Castle, DE, USA) at a heating rate of 5 K min⁻¹ in air atmosphere. Thermal expansion characteristics of the SMP-PTFE powder compacts were recorded by thermomechanical analysis (TMA, model Setsys-1750, Setaram Inc., France), using fused quartz as the push rod. The heating rate was 10 K min⁻¹. The change of appearance of the powder compacts and the contact angle were recorded in situ by an optical contact angle measuring instrument (model OCA20, DataPhysics Instruments GmbH, Filderstadt, Germany). Microstructural analysis was conducted by scanning electron microscopy (SEM, model JSM-5600, Jeol, Tokyo, Japan). The composites were polished, and then coated with an Au film for examination

Results and discussion

3.1 Thermal analyses of the mixed powders

The DTA thermograms of the SMP-PTFE mixed powders are shown in Figure 1a. The enlarged y-scale figure for pure SMP is shown in Figure 1b. As shown in Figure 1b, glass transition ($T_{\rm g} \approx 307\,^{\circ}\text{C}$) and exothermic peaks due to glass crystallization ($T_{\rm Pl} \approx 410~{\rm ^{\circ}C}$ and $T_{\rm Pl} \approx 450~{\rm ^{\circ}C}$) are indicated. As shown in Figure 1a, the PTFE-containing samples reveal a sharp endothermic signal, caused by crystal melting. When the PTFE content is increased, the peak intensity of crystal melting is more obvious, while the peak position is nearly the same (325 °C-327 °C). For pure PTFE, the onset (indicated by ↓) and peak temperature (indicated by •) of the crystal melting signal are 311 °C and 327 °C, respectively. The peak melting temperature of 327 °C is consistent with that reported in some literature.7

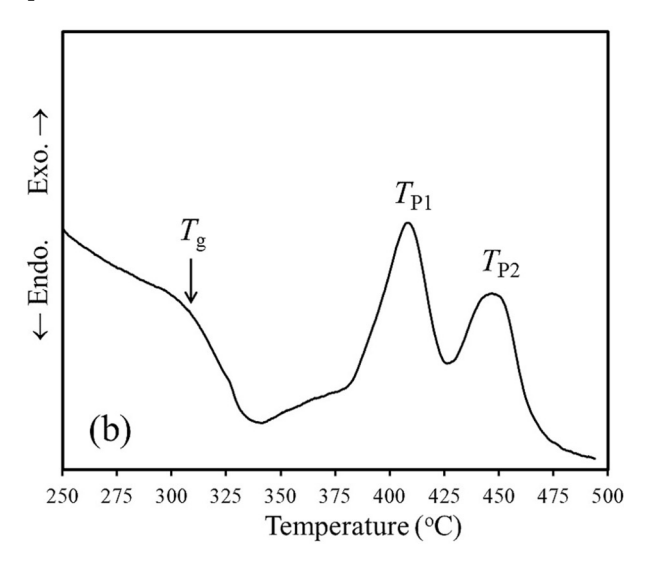
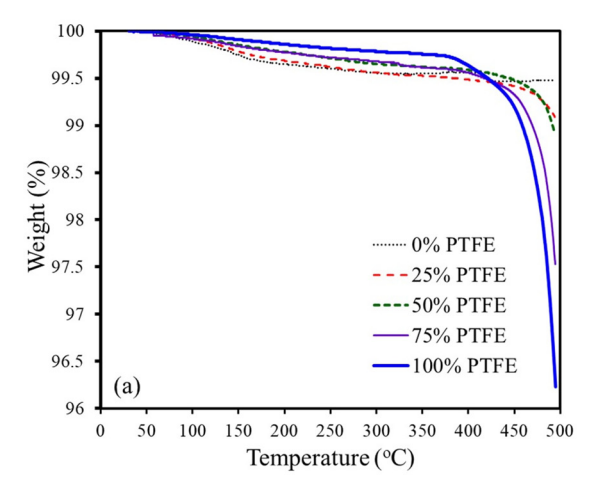


Figure 1: (a) DTA thermograms of the SMP-PTFE mixed powders (1: onset temperature and •: peak temperature of crystal melting). (b) Enlarged y-scale figure for pure SMP.



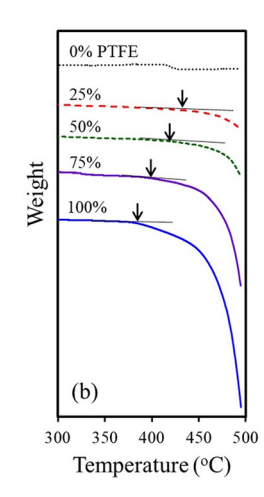


Figure 2: (a) TG thermograms of the SMP-PTFE mixed powders (↓: onset temperature of weight loss). (b) Curves in the range of 300-500 °C in (a) are shifted vertically.

Figure 2a shows the TG thermograms of the mixed SMP-PTFE powders. For pure SMP (i.e., 0 vol.% PTFE), the weight loss is very small, e.g., only 0.5 % near the highest test temperature (500 °C). When PTFE was added, obvious weight reduction was observed in the high temperature range. The weight loss increased from 1.6 wt.% for 25 vol.% (or 16.1 wt.%) PTFE to 2.5 wt.% for 50 vol.% (or 36.6 wt.%) PTFE, 4.5 wt.% for 75 vol.% (or 63.4 wt.%) PTFE, and 6.8 wt.% for pure PTFE near 500 °C. In Figure 2b, these curves are shifted vertically to clearly show the curves of different PTFE contents. The onset temperature of PTFE decomposition (indicated by ↓) decreased from 447 °C for 25 vol.% PTFE to 381 °C for pure PTFE.

Figure 3a shows the thermal-expansion curves of the mixed SMP-PTFE powder compacts. The curve of pure SMP does not show glass transition, possibly because of the powdered form of the sample. Namely, the increase of curve slope at T_{σ} is offset by the increased shrinkage of the powder compact at temperatures near $T_{\rm g}$. In our previous paper, obvious glass transition can be observed for the dense SMP glass.²⁹ As seen in Figure 3a, from room temperature to around 275 °C, in which the curves are nearly linear, the degree of thermal expansion increases generally when the PTFE content was increased (except for 0-25 vol.% PTFE), caused by the intrinsically higher coefficient of thermal expansion (CTE) of PTFE (80 \times 10⁻⁶ K⁻¹, 25 °C-250 °C). The reason for the slightly lower expansion of the 25 vol.% PTFE sample than that of the pure SMP is not clear. It might be caused by the effect of porosity on the thermal expansion.³⁰ At temperatures higher than about 275 °C-300 °C, the curves become nonlinear. Figure 3b Shows the enlarged graph of the high-temperature range in Figure 3a. The pure SMP powder compact begins to soften at around 328 °C,

caused by the reduction in glass viscosity. The pure PTFE powder compact shows a remarkable softening/shrinkage which begins at around 313 °C (indicated by \triangle). The shrinkage possibly resulted from viscous deformation of the glass portion and/or the softening due to crystal melting (onset temperature 311 °C, Figure 1). The expansive peak at 333 °C (indicated by \downarrow) is possibly caused by the increased amount of liquid phase, which has lower density than that of the crystalline phase in PTFE. Unlike pure PTFE, when PTFE was added in SMP, the powder compacts did not shrink before the appearance of expansive peak (indicated by \downarrow). This result possibly resulted from the higher onset-shrinkage temperature (328 °C) of the SMP skeleton than that of pure PTFE (313 °C). The SMP-PTFE mixture begins to soften when the temperature is higher than the expansive peak (around 335 °C-340 °C). It is also noted that the shrinkage rate (i.e., the slope of the curve) in the high temperature region (above 350 °C) increases reasonably with the increasing PTFE content.

Most of the above mentioned characteristic temperatures of SMP glass and PTFE are summarized in Figure 4. It is noted that the onset softening temperatures of SMP (328 °C) and PTFE (313 °C) are close, which are much lower than the onset temperature of weight loss of PTFE (381 °C). This is important for the sintering of SMP-PTFE composites.

3.2 Appearance of the sintered samples

Figure 5a-d shows the in-situ appearance of the pure PTFE sample during continuous heating at a rate of 10 K min⁻¹. As shown in Figure 5a, the region near the sample bottom begins to become transparent at 328 °C, caused by crystal melting (i.e., formation of transparent liquid). This

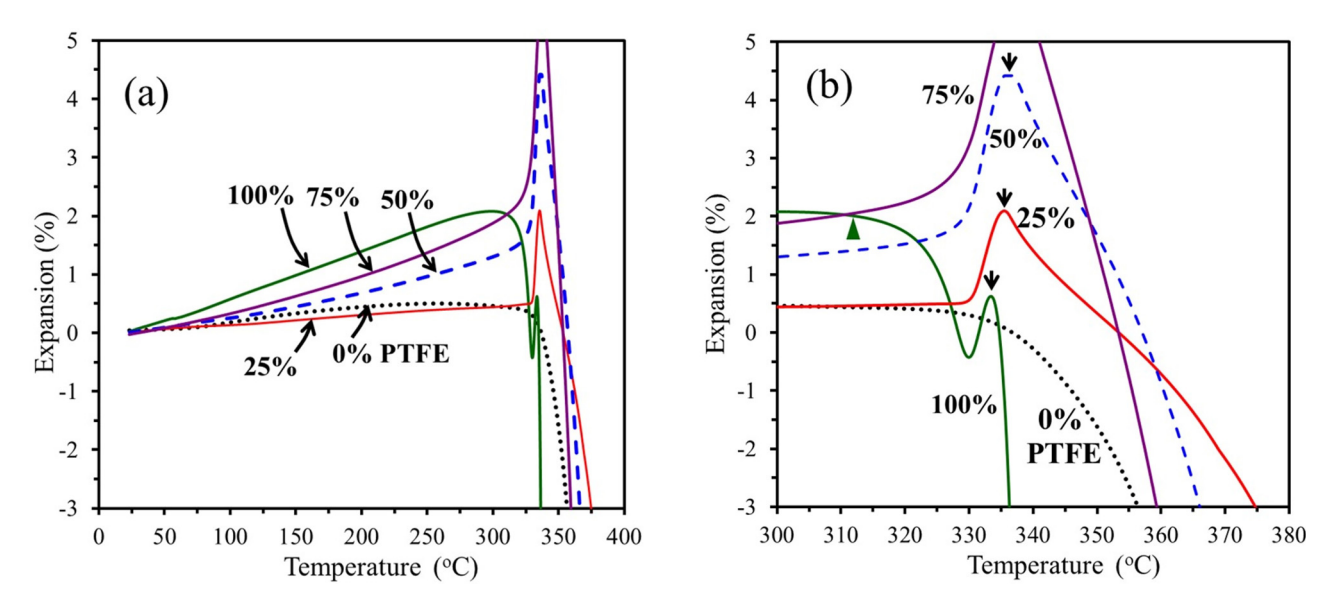


Figure 3: (a) Thermal-expansion curves of the mixed SMP-PTFE powder compacts. (b) Enlarged graph of the high-temperature range in (a).

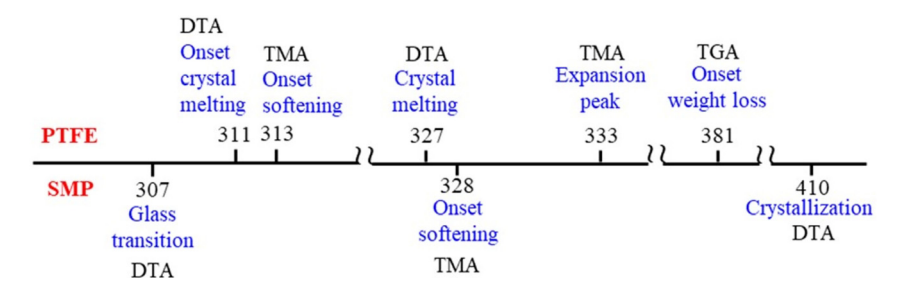


Figure 4: Several characteristic temperatures measured by TG, DTA, and TMA for SMP glass and PTFE.

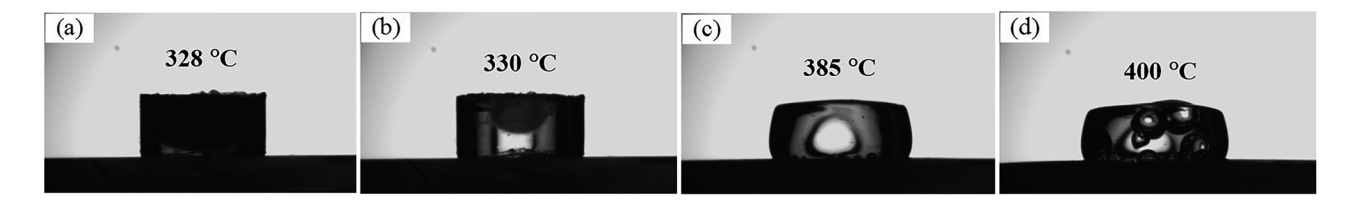


Figure 5: *In-situ* appearance of the PTFE sample during continuous heating at a rate of 10 K min⁻¹.

temperature is consistent with the peak temperature of crystal melting observed in the DTA thermogram (327 °C, Figure 1a or Figure 4). The fraction of transparent region is increased with the increasing temperature (330 °C–385 °C, Figure 5b and c). At 385 °C (Figure 5c), the contour of the sample becomes round and a gas bubble appears due to the decomposition of PTFE. The formation of gas bubbles is in agreement with the onset weight loss observed in the TG thermogram (381 °C, Figures 2 or 4). At 400 °C (Figure 5d), the sample becomes irregular in shape due to the expansion of several gas bubbles.

Figure 6 shows the appearance of the powder compacts containing 0–75 vol.% PTFE sintered at 350 °C–430 °C for 10 min on Corning 1737 glass substrate. For the pure SMP sample, obvious softening occurs at 390 °C. Above 400 °C, the samples reveal a liquid drop contour due to more reduction in glass viscosity. The samples containing 25 vol.% and 50 vol.% PTFE reveal irregular shapes at temperatures higher than 400 °C, resulted from the formation of gas bubbles in the PTFE region (as seen in Figure 5). Increasing the PTFE content to 75 vol.%, this phenomenon occurred at a lower temperature (370 °C).

	Sintering Temperature (°C)					
PTFE content (vol.%)	350	370	390	400	420	430
0					4	
25		1				
50						
75	4	4				_

Figure 6: Appearance of the powder compacts containing 0-75 vol.% PTFE sintered at 350 °C-430 °C for 10 min on Corning 1737[®] glass substrate.

3.3 Sintering of the 1737-[SMP, PTFE]-1737 sandwich structure and its microstructure

The SMP-PTFE powder compacts were further sintered for 10 min at 360 °C-430 °C, placed between an upper and a bottom 1737[®] substrate. It was found that the pure SMP glass is not able to bond to both the upper and bottom substrates, as shown in Figure 7a (the detached 1737[®] substrates are not shown), caused by the large mismatch in CTE $(12.3 \times 10^{-6} \text{ K}^{-1} \text{ and } 3.76 \times 10^{-6} \text{ K}^{-1} \text{ for SMP}^{27} \text{ and } 1737^{\text{?R}})$ respectively). However, the composites containing 25 vol.% PTFE were able to bond to the bottom substrate after sintering at 360 °C. Increasing the sintering temperature to above 370 °C, the composites were able to bond to both the upper and the bottom substrates, as shown in Figure 7b. The pores seen in the PTFE regions of the composite are expected to be a result of grinding and polishing during the preparation of SEM samples, as PTFE is less wear-resistant compared to SMP. When the PTFE content was increased to 75 vol.% and 100 vol.%, the composites are able to bond to

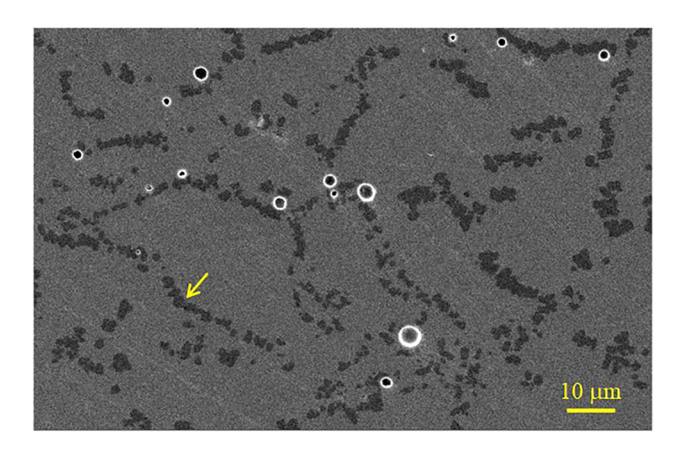
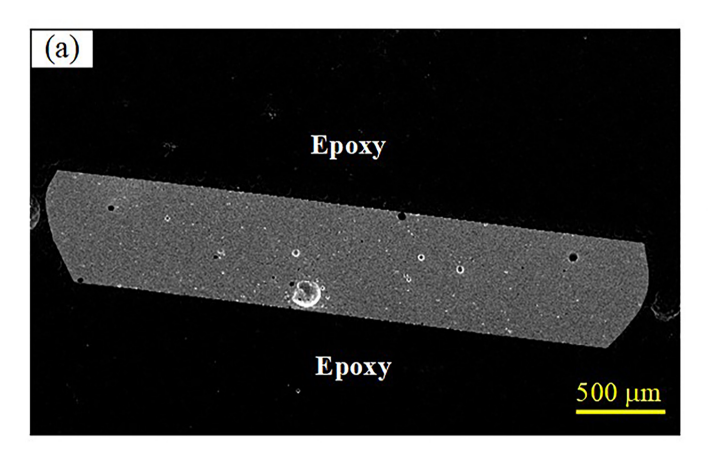


Figure 8: Cross-sectional microstructure for the pure SMP sample shown in Figure 7a. The arrow indicates the crystalline particles formed along the original interfaces between glass particles.

both the upper and the bottom substrates at all sintering temperatures (360 °C-430 °C).

Figure 8 shows the cross-sectional microstructure for the pure SMP sample sintered at 430 °C. The sample did not fully densify and residual pores still remained. The crystalline particles, indicated by the arrow, are possibly MgP2O6, Mg3P2O8, a/o Sn3P2O8 phases.28 It is noted that these crystalline particles do not distribute homogeneously within the glass matrix. Considering the tendency of heterogeneous crystallization of amorphous phase, it is suggested that these crystallites formed along the original interfaces between glass particles (diameter of $37 \mu m-44 \mu m$). The phenomenon has also been discussed in our previous paper.29

The cross-sectional microstructures of the composites with 25 vol.% PTFE sintered at 360 °C-430 °C are shown in Figure 9a-e. Because of the lower amount of PTFE, discrete PTFE regions distribute over the continuous SMP matrix. It



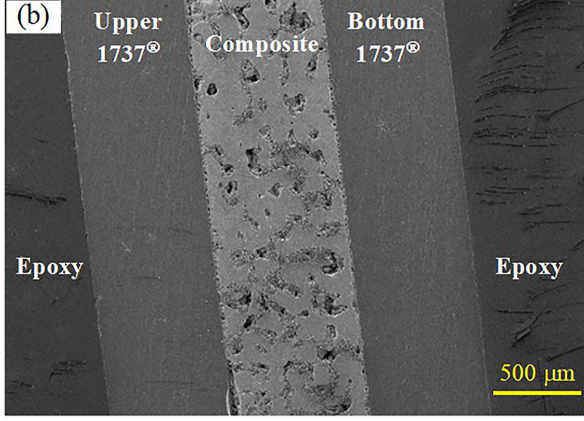


Figure 7: (a) Pure SMP sintered at 430 °C for 10 min and failed to bond to the 1737® substrates. The detached 1737® substrates are not shown. (b) SMP – 25 vol.% PTFE composite sintered at 390 °C for 10 min to bond to the upper and bottom 1737[®] substrates.

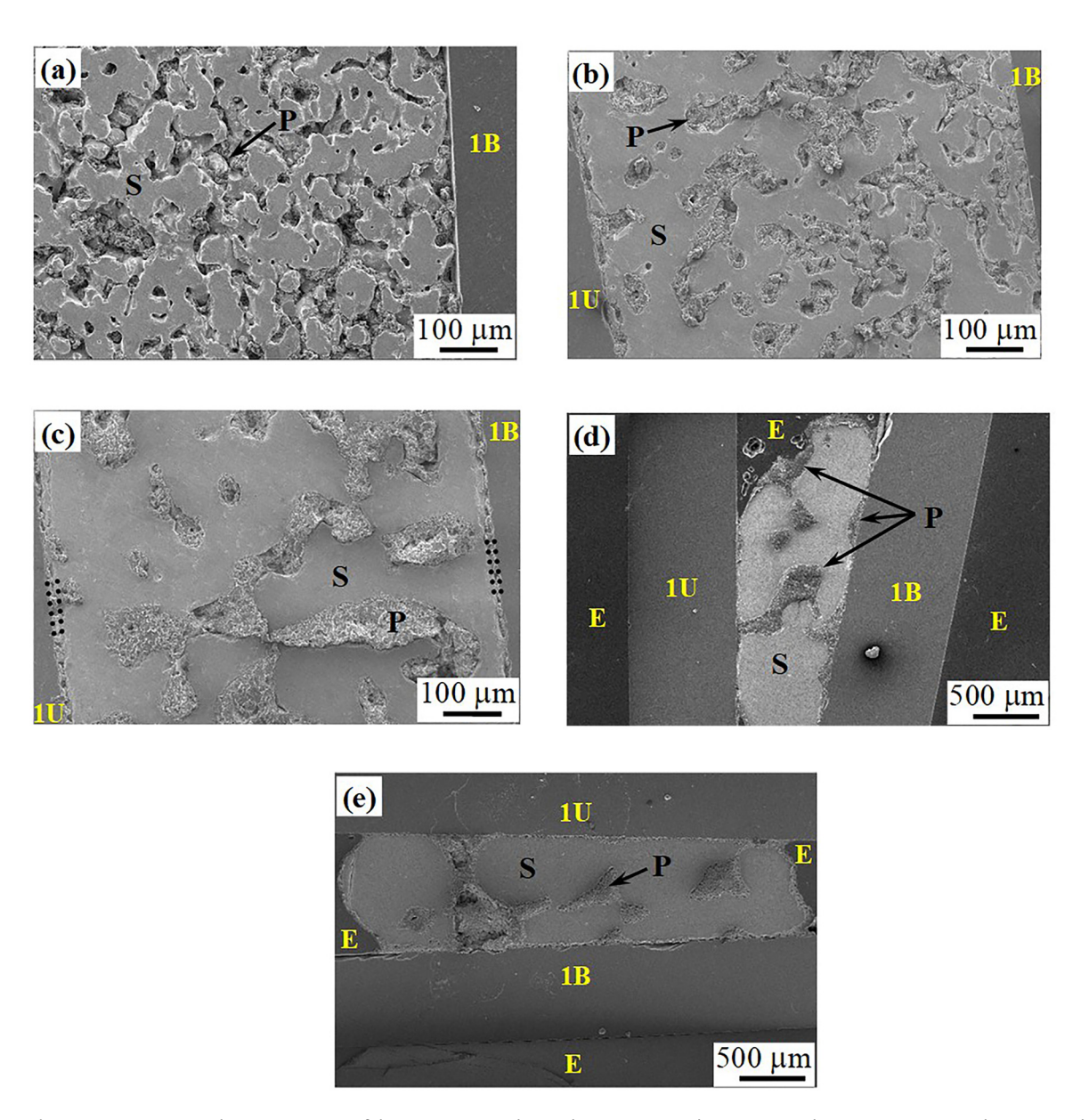


Figure 9: Cross-sectional microstructures of the composites with 25 vol.% PTFE sintered at (a) 360 °C, (b) 380 °C, (c) 390 °C, (d) 420 °C, and (e) 430 °C for 10 min to bond to the upper and bottom 1737® substrates. (S, SMP glass; P, PTFE; 1U, upper substrate; 1B, bottom substrate; E, epoxy).

is noted that the PTFE regions tended to coalescence with the increasing sintering temperature. This result might imply that the interfacial energy between SMP glass and PTFE is high (i.e., high wetting angle). Another possibility is that the SMP matrix became denser with the increasing sintering temperature, the shrinkage of SMP matrix resulted in the coalescence of PTFE.

Above 390 °C (Figure 9c-e), a continuous PTFE thin layer, indicated by the dotted lines in Figure 9c, has developed along the interface between composite and substrate. Figure 10 shows the dependence of the layer thickness on the sintering temperature. It can be seen that the PTFE layer at the bottom interface is thicker that at the upper

interface. The thickness for the upper PTFE layer is about 10-20 µm and shows a weak dependence on the sintering temperature. However, the thickness of the bottom PTFE layer is more sensitive to the sintering temperature, being increased from about 10 μ m to 55 μ m.

Figure 11 shows the contact angle of PTFE on SMP plate, PTFE on 1737[®] plate, and SMP on 1737[®] plate, heated for 10 min at 330 °C, 330 °C/385 °C, and 390 °C/410 °C, respectively. It can be seen that the contact angles of PTFE on both SMP and 1737® have similar values (119° –124°), which are not smaller than the contact angles of SMP on 1737® (74° – 127°). These results indicate that, in comparison with SMP, PTFE did not have a stronger tendency to contact with

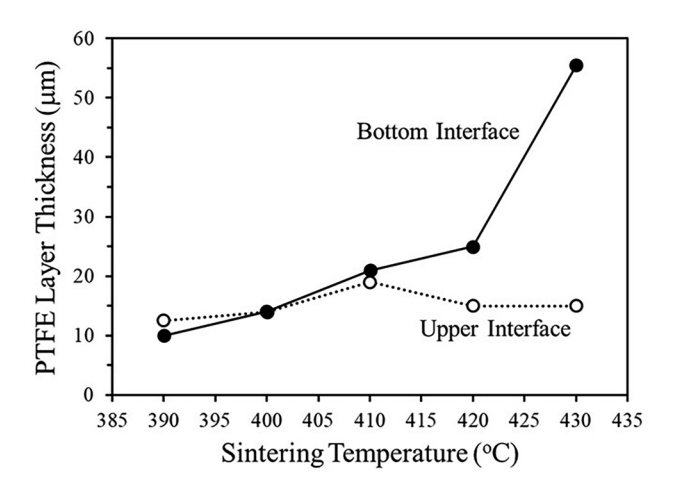


Figure 10: Variation of the thickness of PTFE layer as a function of sintering temperature.

1737® substrate. Therefore, the formation of the PTFE layer between the composite and 1737® substrate might not be connected with surface tension factor. During sintering at temperatures higher than the softening temperature of SMP glass (328 °C, Figures 3 and 4), the SMP glass particles began to densify. The shrinkage force pushes some of the PTFE, which is more flowable than SMP, to accumulate in between composite and substrate. This effect is more remarkable at the higher temperatures (decreased PTFE viscosity) and the lower interface (gravitational force), thus resulting in the thicker PTFE layer, as shown in Figure 10.

Moreover, as previously described, pure SMP was not able to bond with 1737® substrate, while PTFE-containing composites were (e.g., Figures 7 and 9). This result can be explained as follows. Although the difference in CTE between PTFE (80 \times 10⁻⁶ K⁻¹, from Figure 3a) and 1737[®] is larger than that between SMP and 1737[®], the low glass transition temperature (-73 °C) of PTFE promises flowability during cooling after sintering. As a result, the thermal stresses due to CTE mismatch between SMP and 1737® can be partially diminished by the flexibility of PTFE. Moreover, the formation of the PTFE layer is able to remarkably reduce the thermal stresses due to the mismatch in CTE.

When the PTFE content was increased to 50 vol.%, as shown in Figure 12a and b, PTFE becomes the matrix

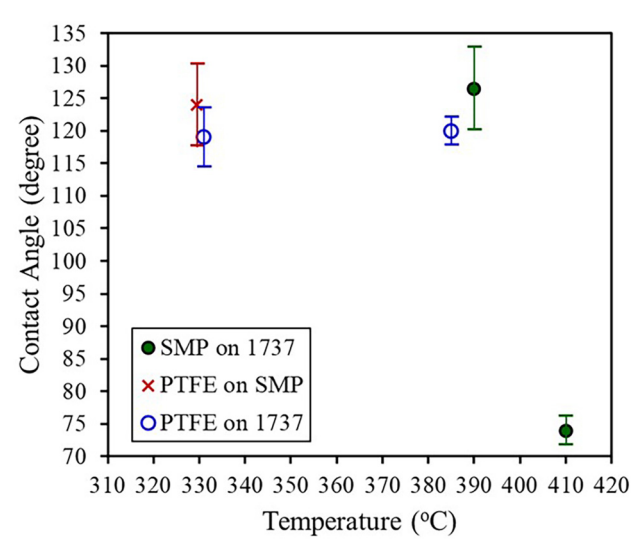


Figure 11: Contact angle of PTFE on SMP plate, PTFE on 1737[®] plate, and SMP on 1737[®] plate, heated for 10 min at 330 °C, 330 °C, and 390 °C/410 °C, respectively.

phase while SMP the discrete regions. Therefore, PTFE is in easy contact with the substrate and no PTFE layer formed between composite and substrate. Moreover, the SMP glass particles became round, resulting from the high interfacial energy. The typical microstructures of the sintered composites with 75 vol.% PTFE (Figure 12c and d for 350 °C and 430 °C, respectively) are similar to that with 50 vol.% PTFE. However, large pores have formed in these samples. Figure 12e and f shows the typical microstructures of the pure PTFE sintered samples. At 330 °C (Figure 12e), the PTFE bonded well with the upper and bottom 1737[®] substrates. However, a huge void formed in the 350 °C-sintered body (Figure 12f).

In summary, pure low- $T_{\rm g}$ SMP glass is not able to bond to the low thermal-expansion 1737® substrate, while the composites containing SMP glass and 25-50 vol.% PTFE are able to bond to the 1737® substrate and show microstructures of low porosity at around 360 °C to below 400 °C. Further increase of the PTFE content to 75-100 vol.% leads to large voids in the microstructure, although the samples are still able to bond to the 1737® substrate. Further work is needed to measure the bond strength of the interfaces between SMP-PTFE and the 1737® glass substrates.

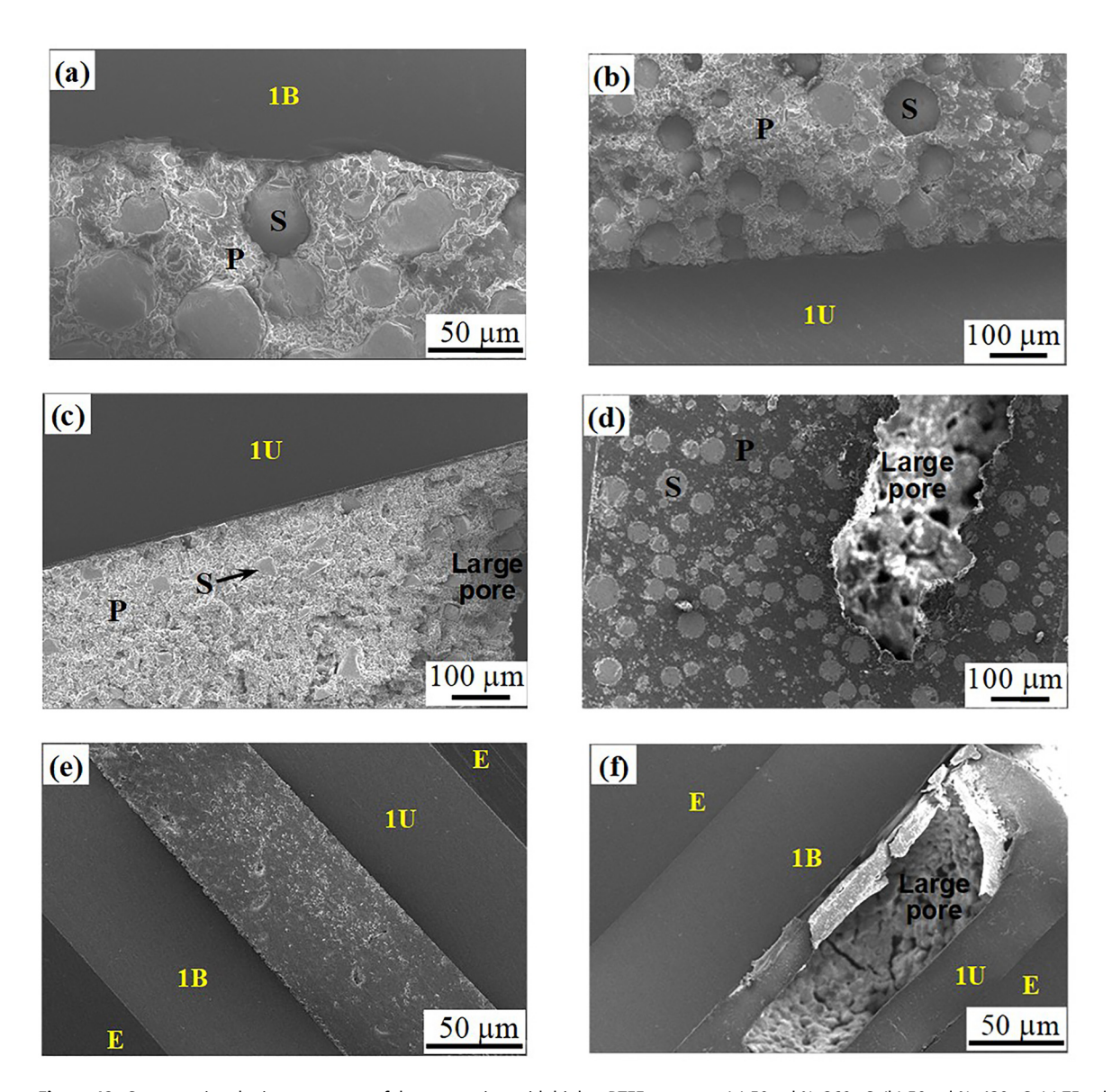


Figure 12: Cross-sectional microstructures of the composites with higher PTFE amounts. (a) 50 vol.%, 360 °C, (b) 50 vol.%, 430 °C, (c) 75 vol.%, 350 °C, (d) 75 vol.%, 430 °C, (e) pure PTFE, 330 °C, and (f) pure PTFE, 350 °C. Sintering time 10 min. S, SMP glass; P, PTFE; 1U, upper substrate; 1B, bottom substrate; E, epoxy.

4 Conclusions

Composites containing an SnO–MgO– P_2O_5 (SMP) glass and polytetrafluoroethylene (PTFE) were fabricated by a sintering route. Influences of SMP:PTFE ratio and sintering temperature (350 °C–430 °C) on the formation of composite and bonding ability to Corning 1737 $^{\circledR}$ glass substrate were investigated. The following results have emerged:

(1) The onset temperature for dilatometric softening is 328 °C and 313 °C for SMP glass and PTFE, respectively. Pure PTFE shows an expansive peak at 333 °C. The SMP-PTFE powder compacts begin to soften

- when the temperature is higher than the expansive peak (around 335 °C-340 °C). The onset temperature of weight loss of PTFE (381 °C) is much higher than both the onset softening temperatures of SMP and PTFE (328 °C and 313 °C). This is important for the sintering of SMP-PTFE composites.
- (2) After sintering, pure SMP glass was not able to bond to the low thermal-expansion 1737[®] glass substrates. However, SMP-PTFE composites were able to bond to 1737[®] after sintering at appropriate temperatures. It is suggested that thermal stresses due to thermal-expansion mismatch between the composite

- and 1737® can be partially diminished by the flexibility of PTFE and the formation of PTFE layer at the composite-1737® interfaces.
- For the composites containing 25 vol.% PTFE, the formation of a PTFE layer between composite and substrate might be caused by the shrinkage force due to SMP sintering, pushing some of the viscous PTFE to accumulate in between composite and substrate.
- For composites containing less PTFE (25 vol.%), discrete PTFE regions distribute over the continuous SMP matrix. When the PTFE content was increased to 50 vol.%, PTFE becomes the matrix phase while SMP the discrete regions. Higher amounts of PTFE (>75 vol.%) resulted in large pores which will weaken the composite-substrate interfaces.
- The composites containing the low- $T_{\rm g}$ SMP glass and 25-50 vol.% PTFE are able to bond to the low thermalexpansion 1737® glass substrate and show microstructures of low porosity at around 360 °C to below 400 °C.

Research ethics: Not applicable.

Author contributions: The authors have accepted responsibility for the entire content of this manuscript and approved its submission. In addition, the individual contributions of each author are outlined below: J.J. Shyu: supervision, conceptualization, methodology, formal analysis, writingreview and editing, funding acquisition. P.C. Tsai: investigation, data curation, writing-original draf preparation.

Competing interests: The authors states no competing interests.

Research funding: This work was supported by National Science and Technology Council (Taiwan) under Contract No. NSC 95-2221-E-036-017. It was also supported by Tatung University under Contract No. B95-T04-075.

Data availability: The raw data can be obtained on request from the corresponding author.

References

- 1. Hudecek, C. J. Engineered Materials Handbook, Vol. 4; ASM International, Materials Park: Ohio, USA, 1991; p 1069.
- 2. Geodakyan, D. A.; Petrosyan, B. V.; Stepanyan, S. V.; Geodakyan, K. D. Glass Ceram. 2009, 66, 381-384. https://doi.org/10.1007/ s10717-010-9206-7.
- 3. Morena, R. J. Non-Cryst. Solids 2000, 263-264 (1), 382-387. https://doi.org/10.1016/S0022-3093(99)00678-X.
- 4. Morena, R. Fusion Seal and Sealing Mixtures. US Patent, 2000;
- 5. Ticha, H.; Kincl, M.; Tichy, L. Mater. Chem. Phys. 2013, 138, 633-639. https://doi.org/10.1016/j.matchemphys.2012.12.032.

- 6. Naito, T.; Aoyagi, T.; Sawai, Y.; Tachizono, S.; Yoshimura, K.; Hashiba, Y.; Yoshimoto, M. Jpn. J. Appl. Phys. 2011, 50 (8R), 088002. https://doi.org/10.1143/JJAP.50.088002.
- 7. Christakopoulos, F.; Troisi, E.; Tervoort, T. A. Polymers 2020, 12 (4), 791. https://doi.org/10.3390/polym12040791.
- 8. Blumm, J.; Lindemann, A.; Meyer, M.; Strasser, C. Int. J. Thermophys. 2010, 31, 1919-1927. https://doi.org/10.1007/s10765-008-0512-z.
- 9. Purser, D. A. Fire Mater. 1992, 16 (2), 67-75. https://doi.org/10 .1002/fam.810160204.
- 10. Wall, L. A.; Michaelsen, J. D. J. Res. Natl. Bur. Stand. 1956, 56 (1), 27-34. https://doi.org/10.6028/jres.056.004.
- 11. Küchler, A. High Voltage Engineering: Fundamentals-Technology-Applications; Springer Vieweg: Berlin, Germany, 2018; pp 311-316.
- 12. Teflon PTFE Properties Handbook; Dupont: Wilmington, Delaware,
- 13. Bur, A. J. Polym. 1985, 26 (7), 963-977. https://doi.org/10.1016/ 0032-3861(85)90216-2.
- 14. Gupta, K. M.; Gupta, N. Advanced Electrical and Electronics Materials: Processes and Applications; Wiley-Scrivener: Salem, Massachusetts, USA, 2015; pp 503-507.
- 15. Ashokbabu, A.; Thomas, P. 2019 IEEE 4th International Conference on Condition Assessment Techniques in Electrical Systems (CATCON): Chennai, India, 2019; pp 1-4.
- 16. Jiang, P.; Bian, J. Int. J. Appl. Ceram. Technol. 2018, 16 (1), 152-159. https://doi.org/10.1111/ijac.13083.
- 17. Alhaji, I. A.; Abbas, Z.; Zaid, M. H. M.; Zainuddin, N. J. Solid State Sci. Technol. Lett. **2022**, 23 (1-2), 29-34.
- 18. Yuan, Y.; Zhang, S. R.; Zhou, X. H.; Li, E. Z. Mater. Chem. Phys. 2013, 141 (1), 175-179. https://doi.org/10.1016/j.compositesb.2018.07
- 19. Wu, K. T.; Yuan, Y.; Zhang, S. R.; Yan, X. Y.; Cui, Y. R. J. Polym. Res. 2013, 20, 223. https://doi.org/10.1007/s10965-013-0223-4.
- 20. Yuan, Y.; Cui, Y. R.; Wu, K. T.; Huang, Q. Q.; Zhang, S. R. J. Polym. Res. 2014, 21, 366. https://doi.org/10.1007/s10965-014-0366-y.
- 21. Rajesh, S.; Murali, K. P.; Priyadarsini, V.; Potty, S. N.; Ratheesh, R. Mater. Sci. Eng. B 2009, 163 (1), 1-7. https://doi.org/10.1016/j.mseb .2009.04.011.
- 22. Yuan, Y.; Lin, H.; Yu, D.; Yin, Y.; Tang, B.; Li, E.; Zhang, S. J. Mater. Sci.: Mater. Electron. 2017, 28 (12), 8810 — 8817. https://doi.org/10 .1007/s10854-017-6608-0.
- 23. Luo, F.; Tang, B.; Yuan, Y.; Fang, Z.; Zhang, S. Appl. Surf. Sci. 2018, 456, 637-644. https://doi.org/10.1016/j.apsusc.2018.06.204.
- 24. Wang, H.; Yang, H.; Wang, Q.; Tong, J.; Wen, J.; Zhang, Q. Compos. Commun. 2020, 22, 100523. https://doi.org/10.1016/j.coco.2020
- 25. Gorshkov, N.; Goffman, V.; Vikulova, M.; Burmistrov, I.; Sleptsov, V.; Gorokhovsky, A. J. Appl. Polym. Sci. 2020, 137 (22), 48762. https:// doi.org/10.1002/app.48762.
- 26. Ndayishimiye, A.; Tsuji, K.; Wang, K.; Bang, S. H.; Randall, C. A. J. Eur. Ceram. Soc. 2019, 39 (15), 4743-4751. https://doi.org/10.1016/j .jeurceramsoc.2019.07.048.
- 27. Shyu, J. J.; Yeh, C. H. J. Mater. Sci. 2007, 42 (13), 4772 4777. https:// doi.org/10.1007/s10853-006-0766-4.
- 28. Shyu, J. J.; Yeh, C. H. J. Mater. Sci. 2011, 46 (4), 999-1006. https:// doi.org/10.1007/s10853-010-4861-1.
- 29. Shyu, J. J.; Lin, W. Y. J. Ceram. Soc. Jpn. 2012, 120 (8), 324-329. https://doi.org/10.2109/jcersj2.120.324.
- 30. Ghabezloo, S. Constr. Build. Mater. 2010, 24 (9), 1796-1798. https:// doi.org/10.1016/j.conbuildmat.2010.03.006.